Structural Diversity in Solvated Lithium Aryloxides. Syntheses, Characterization, and Structures of $[Li(OAr)(THF)_x]_n$ and $[Li(OAr)(py)_x]_2$ Complexes Where OAr = OC_6H_5, OC_6H_4(2-Me), OC_6H_3(2,6-(Me))$_2$, OC_6H_4(2-Pr^i), OC_6H_3(2,6-(Pr^i))$_2$, OC_6H_4(2-Bu^t), OC_6H_3(2,6-(Bu^t))$_2$

Timothy J. Boyle,* Dawn M. Pedrotty, Todd M. Alam, Sara C. Vick, and Mark A. Rodriguez

Sandia National Laboratories, Advanced Materials Laboratory, 1001 University Boulevard SE, Albuquerque, New Mexico 87106

Received April 19, 2000

A series of sterically varied aryl alcohols H−OAr [OAr = OC_6H_5 (OPh), OC_6H_4(2-Me) (oMP), OC_6H_3(2,6-(Me))$_2$ (DMP), OC_6H_4(2-Pr^i) (oPP), OC_6H_3(2,6-(Pr^i))$_2$ (DIP), OC_6H_4(2-Bu^t) (oBP), OC_6H_3(2,6-(Bu^t))$_2$ (DBP); Me = CH_3, Pr^i = $CHMe_2$, and Bu^t = CMe_3] were reacted with $LiN(SiMe_3)_2$ in a Lewis basic solvent [tetrahydrofuran (THF) or pyridine (py)] to generate the appropriate "$Li(OAr)(solv)_x$". In the presence of THF, the OPh derivative was previously identified as the hexagonal prismatic complex $[Li(OPh)(THF)]_6$; however, the structure isolated from the above route proved to be the tetranuclear species $[Li(OPh)(THF)]_4$ (**1**). The other "$Li(OAr)(THF)_x$" products isolated were characterized by single-crystal X-ray diffraction as $[Li(OAr)(THF)]_4$ [OAr = oMP (**2**), DMP (**3**), oPP (**4**)], $[Li(DIP)(THF)]_3$ (**5**), $[Li(oBP)(THF)_2]_2$, (**6**), and $[Li(DBP)(THF)]_2$, (**7**). The tetranuclear species (**1**−**4**) consist of symmetric cubes of alternating tetrahedral Li and pyramidal O atoms, with terminal THF solvent molecules bound to each metal center. The trinuclear species **5** consists of a six-membered ring of alternating trigonal planar Li and bridging O atoms, with one THF solvent molecule bound to each metal center. Compound **6** possesses two Li atoms that adopt tetrahedral geometries involving two bridging oBP and two terminal THF ligands. The structure of **7** was identical to the previously reported $[Li(DBP)(THF)]_2$ species, but different unit cell parameters were observed. Compound **7** varies from **6** in that only one solvent molecule is bound to each Li metal center of **7** because of the steric bulk of the DBP ligand. In contrast to the structurally diverse THF adducts, when py was used as the solvent, the appropriate "$Li(OAr)(py)_x$" complexes were isolated as $[Li(OAr)(py)_2]_2$ (OAr = OPh (**8**), oMP (**9**), DMP (**10**), oPP (**11**), DIP (**12**), oBP (**13**)) and $[Li(DBP)(py)]_2$ (**14**). Compounds **8**−**13** adopt a dinuclear, edge-shared tetrahedral complex. For **14**, because of the steric crowding of the DBP ligand, only one py is coordinated, yielding a dinuclear fused trigonal planar arrangement. Two additional structure types were also characterized for the DIP ligand: $[Li(DIP)(H\text{-}DIP)(py)]_2$ (**12b**) and $[Li_2(DIP)_2(py)_3]$ (**12c**). Multinuclear (^{6,7}Li and ^{13}C) solid-state MAS NMR spectroscopic studies indicate that the bulk powder possesses several Li environments for "transitional ligands" of the THF complexes; however, the py adducts possess only one Li environment, which is consistent with the solid-state structures. Solution NMR studies indicate that "transitional" compounds of the THF precursors display multiple species in solution whereas the py adducts display only one lithium environment.

Introduction

Metal alkoxides have been extensively used, with a great deal of success, as precursors to ceramic materials. To generate higher quality materials with controlled stoichiometries, mixed-metal alkoxides are of interest. These "single-source" precursors can be generated through the introduction of a metathesizable cations such as alkali metals:[1−6]

$$A(OR) + Ti(OR)_4 \xrightarrow{\text{toluene}} {}^1/_n[ATi(OR)_5]_n \qquad (1)$$

$$[ATi(OR)_5]_n + nMCl_x \xrightarrow{\text{toluene}} \text{“}MTi(OR)_5(Cl)_{x-n}\text{”} + nACl \qquad (2)$$

Unfortunately, the reaction does not always proceed as written and retention of the alkali metals or halide atoms is often observed. To understand this phenomenon, we previously characterized the mixed-metal precursors $[ATi(OR)_5]_n$, where A = Li, Na, or K; OR = $OCHMe_2$ or OCH_2CMe_3; and $n = 2$ or ∞.[5,6] It was thought that the alkali metal cation and the "$Ti(OR)_5^-$" anion were tight ion pairs in solution, which did not allow for successful removal of the alkali metal. For reaction 1, only the $Ti(OR)_4$ precursors have been extensively characterized.[7] However, the "simplistically" written A(OR) precursors are often more complex than is realized.[8−23] For this study

* To whom correspondence should be sent.

(1) Bradley, D. C.; Mehrotra, R. C.; Gaur, D. P. *Metal Alkoxides*; Academic Press: New York, 1978.
(2) Hubert-Pfalzgraf, L. G. *New. J. Chem.* **1987**, *11*, 663.
(3) Bradley, D. C. *Chem. Rev.* **1989**, *89*, 1317.
(4) Chandler, C. D.; Roger, C.; Hampden-Smith, M. J. *Chem. Rev.* **1993**, *93*, 1205.
(5) Boyle, T. J.; Alam, T. M.; Tafoya, C. J.; Mechenbeir, E. R.; Ziller, J. W. *Inorg. Chem.* **1999**, *38*, 2422.
(6) Boyle, T. J.; Bradley, D. C.; Hampden-Smith, M. J.; Patel, A.; Ziller, J. W. *Inorg. Chem.* **1995**, *34*, 5893.
(7) Boyle, T. J.; Alam, T. M.; Mechenbeir, E. R.; Scott, B.; Ziller, J. W. *Inorg. Chem.* **1997**, *36*, 3293.
(8) Beck, G.; Hitchcock, P. B.; Lappert, M. F.; Mackinnon, I. A. *J. Chem. Soc., Chem. Commun.* **1989**, 1312.

10.1021/ic000432a CCC: $19.00
Published on Web 10/10/2000

we have focused on understanding the structural characteristics of lithium alkoxide [Li(OR)] compounds.

Lithium derivatives of organic compounds [i.e., alkyl ($-CR_3$), alkoxide ($-OR$), amide ($-NR_2$), and halide ($-X$)] have been investigated in great detail, with many of these compounds being crystallographically characterized.[24,25] From these studies, it has been garnered that the structural motifs of the Li complexes typically aggregate, forming at least 12 general structural types.[24] The factors that determine the final structure adopted by these compounds have been attributed to a number of characteristics, including the choice of solvent (Lewis basicity) used to synthesize these compounds, the electron-donating ability of the α atom of the ligand (C, N, O, or X), the bonding ability of the ligand (mono-, bi-, tri-, or polydentate), and/or the steric bulk and number of pendant hydrocarbon chains ($-X$, $-OR$, $-NR_2$, $-CR_3$).[24,25] This "flexibility" often leads to confusion concerning the structural properties of the final lithiated precursors. Therefore, to fully exploit and understand the reactivity of the Li(OR) precursors, it is necessary to structurally identify these compounds.

Our studies have further focused on the lithium adducts of aryl alcohols H−OAr [OAr = OC_6H_5 (OPh), OC_6H_4(2-Me) (oMP), OC_6H_3(2,6-(Me))$_2$ (DMP), OC_6H_4(2-Pr^i) (oPP), OC_6H_3-(2,6-(Pr^i))$_2$ (DIP), OC_6H_4(2-Bu^t) (oBP), OC_6H_3(2,6-(Bu^t))$_2$ (DBP); Me = CH_3, Pr^i = $CHMe_2$, and Bu^t = CMe_3] due to the systematic variations of ring substituents that are readily available. Changes in the ortho substituent of the phenoxide ring were investigated because the steric bulk in this position would have the greatest influence over the final Li(OAr) structure. We have synthesized a series of Li(OAr) compounds in different solvents through the amide alcohol exchange reaction shown in eq 3. Our initial investigations utilized tetrahydrofuran (THF) as the Lewis basic solvent. The structure of the unhindered OPh was previously reported as [Li(OPh)-(THF)]$_6$,[17] and the sterically hindered DBP was found to adopt a dinuclear arrangement, [Li(DBP)(THF)]$_2$.[13] Our investigation of sterically varied Li(OAr) in THF led to the isolation of [Li-(OAr)(THF)]$_4$ [OAr = OPh (**1**), oMP (**2**), DMP (**3**), oPP (**4**)], [Li(DIP)(THF)]$_3$ (**5**), [Li(oBP)(THF)$_2$]$_2$ (**6**), and [Li(DBP)-(THF)]$_2$ (**7**). Since solvent effects have also been reported to yield structural variations of Li−X compounds, we further investigated structural variations of Li(OAr) in the presence of a stronger Lewis basic solvent, pyridine (py). The resultant products isolated from eq 3 using py were identified as [Li-

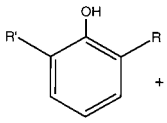

$$+\ LiN(SiMe_3)_2 \xrightarrow{solv} 1/n\ [Li(OAr)(solv)_x]_n + HN(SiMe_3)_2 \quad (3)$$

			THF			py		
OAr	R	R'	Cmpd	n	x	Cmpd	n	x
OPh	H	H	**1**	6	1	**8**	2	2
oMP	Me	H	**2**	4	1	**9**	2	2
DMP	Me	Me	**3**	4	1	**10**	2	2
oPP	Pr^i	H	**4**	4	1	**11**	2	2
DIP	Pr^i	Pr^i	**5**	3	1	**12**	2	2
oBP	Bu^t	H	**6**	2	2	**13**	2	2
DBP	Bu^t	Bu^t	**7**	2	1	**14**	2	1

(OAr)(py)$_2$]$_2$ [OAr = OPh (**8**), oMP (**9**), DMP (**10**), oPP (**11**), DIP (**12**), oBP (**13**)] and [Li(DBP)(py)]$_2$ (**14**). Two additional compounds were observed for the DIP ligand: [Li(DIP)(H-DIP)-(py)]$_2$ (**12b**) and [Li$_2$(DIP)$_2$(py)$_3$] (**12c**). Solid- and solution-state multinuclear NMR spectroscopy were used to determine the properties and structural aspects of the solvated adducts of Li(OAr) complexes. Details of the syntheses and characterization of these compounds are presented below and in Supporting Information.

Experimental Section

All compounds were handled with rigorous exclusion of air and water, using standard Schlenk line and glovebox techniques. All solvents were freshly distilled from the appropriate drying agent immediately prior to use.[26] The following chemicals were used as received (Aldrich), stored, and handled under an argon atmosphere: H−OPh, H-oMP, H-DMP, H-oPP, H-DIP, H-oBP, H-DBP, and LiN(SiMe$_3$)$_2$. Analytical data was collected on crystalline material, under inert conditions, as described in the supplemental information.

General Synthesis. To a solution of LiN(SiMe$_3$)$_2$ in the appropriate Lewis basic solvent (THF or py), the HOAr was added with stirring. After 12 h, the volatile portion of the reaction mixture was removed by rotary evaporation to drastically reduce the volume of the solution. The reaction mixture was allowed to sit for several hours at glovebox temperatures until X-ray-quality crystals formed, which were used for all subsequent analyses. Bulk powder yields were quantitative, but crystalline yields were not optimized. Additional details, including preparatory scale, FT-IR spectra, solution NMR (^{1}H, ^{13}C, ^{7}Li) data, and elemental analyses of **1**−**14** can be found in Supporting Information.

General X-ray Crystal Structure Information. All crystals were mounted onto a thin glass fiber from a pool of Fluorolube and immediately placed under a liquid N_2 stream, on a Bruker AXS diffractometer. The radiation used was graphite monochromatized Mo Kα radiation (λ = 0.7107 Å). The lattice parameters were optimized from a least-squares calculation on carefully centered reflections. Lattice determination and data collection were carried out using SMART, version 5.054, software.[27] Data reduction was performed using SAINT, version 6.01, software.[27] The structure refinement was performed using XSHELL 3.0 software.[27] The data were not corrected for absorption because of the low absorption coefficient. Each structure was solved using direct methods that yielded the Li and O atoms, along with a number of the C atoms. Subsequent Fourier synthesis yielded the remaining C atom positions. The hydrogen atoms were fixed in positions of ideal geometry and refined within the XSHELL software.[27] These idealized hydrogen atoms had their isotropic temperature factors fixed

(9) Cetinkaya, B.; Gumrukcu, I.; Lappert, M. F.; Atwood, J. L.; Shakir, R. *J. Am. Chem. Soc.* **1980**, *102*, 2086.
(10) Chisholm, M. H.; Drake, S. R.; Naiini, A. A.; Streib, W. E. *Polyhedron* **1991**, *10*, 805.
(11) Goldfuss, B.; Schleyer, P. V. R.; Hampel, F. *J. Am. Chem. Soc.* **1996**, *118*, 12183.
(12) Goldfuss, B.; Schleyer, P. V. R.; Hampel, F. *J. Am. Chem. Soc.* **1997**, *119*, 1072.
(13) Huffman, J. C.; Geerts, R. L.; Caulton, K. G. *J. Crystallogr. Spectrosc. Res.* **1984**, *14*, 541.
(14) Hvoslef, J.; Hope, H.; Murray, B. D.; Power, P. P. *J. Chem. Soc., Chem. Commun.* **1983**, 1438.
(15) Jackmann, L. M.; Debrosse, C. W. *J. Am. Chem. Soc.* **1983**, *105*, 4177.
(16) Jackmann, L. M.; Smith, B. D. *J. Am. Chem. Soc.* **1988**, *110*, 3829.
(17) Jackmann, L. M.; Cizmeciyan, D.; Williard, P. G.; Nichols, M. A. *J. Am. Chem. Soc.* **1993**, *115*, 6262.
(18) Kociok-Kohn, G.; Pickardt, J.; Shumann, H. *Acta Crystallogr.* **1991**, *C47*, 2649.
(19) Thiele, K.; Goerls, H.; Seidel, W. *Z. Anorg. Allg. Chem.* **1998**, *624*, 1391.
(20) Williard, P. G.; Carpenter, G. B. *J. Am. Chem. Soc.* **1985**, *107*, 3345.
(21) Williard, P. G.; Carpenter, G. B. *J. Am. Chem. Soc.* **1986**, *108*, 462.
(22) Williard, P. G.; MacEwan, G. J. *J. Am. Chem. Soc.* **1989**, *111*, 7671.
(23) Wheatley, P. J. *J. Chem. Soc.* **1960**, 4270.
(24) Pauer, F.; Power, P. P. Structures of Lithium Salts of Heteroatom Compounds. In *Lithium Chemistry. A Theoretical and Experimental Overview*; Sapse, A.-M., Schleyer, P. V. R., Eds.; John Wiley & Sons: New York, 1995; p 295 and references therein.
(25) Sapse, A.-M.; Jain, D. C.; Rahgavachari, K. *Theoretical Studies of Aggregates of Lithium Compounds* in *Lithium Chemistry. A Theoretical and Experimental Overview*; Sapse, A.-M., Schleyer, P. V. R., Eds.; John Wiley & Sons: New York, 1995; p 45 and references therein.
(26) Perrin, D. D.; Armarego, W. L. F. *Purification of Laboratory Chemicals*, 3rd ed.; Pergamon Press: New York, 1988.
(27) The listed versions of SAINT, SMART, XSHELL Software from Bruker Analytical X-Ray Systems Inc., 6300 Enterprise Lane, Madison, WI 53719 were used in analysis.

Table 1. Data Collection Parameters for **1**−**7**

compound	**1**	**2**	**3**	**4**	**5**	**6**	**7**
chemical formula	$C_{20}H_{26}Li_2O_4$	$C_{44}H_{60}Li_4O_8$	$C_{48}H_{68}Li_4O_8$	$C_{52}H_{76}Li_4O_8$	$C_{48}H_{75}Li_3O_6$	$C_{18}H_{29}LiO_3$	$C_{36}H_{58}Li_2O_4$
fw	344.29	744.68	800.78	856.89	768.90	300.35	568.70
temp (K)	168	168	168	293	168	168	168
space group	monoclinic *C*2/*c*	monoclinic *P*2$_1$/*c*	monoclinic *P*2$_1$/*n*	monoclinic *P*2$_1$/*c*	monoclinic *P*2$_1$/*n*	monoclinic *P*2$_1$/*n*	monoclinic *P*2$_1$/*n*
a (Å)	26.890(3)	16.187(7)	12.562(1)	12.946(2)	13.316(2)	9.1510(7)	12.483(3)
b (Å)	9.2373(9)	14.941(7)	20.819(3)	15.119(2)	16.148(3)	14.4287(12)	14.693(4)
c (Å)	19.761(2)	18.920(10)	17.135(2)	27.015(4)	22.427(3)	14.1346(12)	20.207(5)
β (deg)	124.81(1)	108.43(1)	91.77(1)	101.01(1)	90.00(1)	105.32(1)	107.993(4)
V (Å^3)	4030(1)	4341(4)	4479(1)	5190(1)	4822(1)	1800(1)	3525(1)
Z	8	4	4	4	4	4	4
D_{calcd} (Mg/m^3)	1.135	1.139	1.187	1.097	1.059	1.108	1.072
μ (Mo Kα) (mm^{-1})	0.076	0.075	0.077	0.070	0.066	0.072	0.066
R1[a] ([$I > 2\sigma(I)$], %)	5.41	8.64	9.01	8.59	6.26	5.27	5.76
wR2[b] ([$I > 2\sigma(I)$], %)	12.52	27.60	24.80	23.24	15.66	14.71	12.89
R1[a] (all data, %)	15.70	19.00	11.12	17.93	26.20	9.16	17.14
wR2[b] (all data, %)	15.82	30.87	27.68	29.24	21.79	17.24	16.73

[a] $R1 = \sum||F_o| - |F_c||/\sum|F_o| \times 100$. [b] $wR2 = [\sum w(F_o^2 - F_c^2)^2/\sum(w|F_o|^2)^2]^{1/2} \times 100$.

at 1.2 or 1.5 times the equivalent isotropic U of the C atoms they were bonded to. The final refinement of each compound included anisotropic thermal parameters on all non-hydrogen atoms. Additional information concerning the data collection and final structural solutions of **1**−**14** can be found in Supporting Information.

Results and Discussion

Lithium alkoxides have been structurally characterized in aggregate forms that range from mononuclear [using polydentate donor molecules (i.e., crown ethers)] to dinuclear (most frequently observed) to trinuclear (rare) to tetranuclear (cubes) to hexanuclear (hexagonal prisms) to polymeric; however, most of these compounds utilize "complex" multidentate or heteroatomic alkoxide-like pendant chains.[24,25] A list of "simple" lithium alkoxide (OR) or aryloxide (OAr) species that have been crystallographically characterized would include $[Li(OMe)]_\infty$,[22,23] $[Li(OCBu^t_3)(THF)]_2$,[14] $[Li(OCBu^t_3)]_2$,[8] $[Li(OCBu^t{=}CH_2)(THF)]_4$,[21] $[Li(OCMe_2Ph)]_6$,[10] $[Li(OC(Me){=}CMe_3]_6$,[20] $[Li(OCMe_2{-}C{\equiv}C{-}H)]_6$,[12] $Li(OC(Me)(c\text{-}CHCH_2CH_2)_2]_6$,[11] and OAr = $[Li(OC_6H_2(4\text{-}Me)(2,6\text{-}(Bu^t))_2(OEt_2)]_2$,[9] $[Li(OC_6H_3(2,6\text{-}(Bu^t))_2(solv)]_2$ (solv = OEt_2[18] and THF[13]), $[Li(OC_6H_2(2,4,6\text{-}(Me))_3]_4(THF)_3$,[19] and $[Li(OC_6H_5)(THF)]_6$.[17] While the number of Li(OR) compounds that have been structurally characterized is plentiful, little systematic investigation concerning the solid-state structure of these compounds has been forthcoming. Because of the continued interest in Li(OR) for use as metathesizable reagents and the variability of steric bulk readily available with the OAr ligands, we have synthesized and characterized a series of "Li(OAr)(solv)$_x$" with increased steric bulk in the ortho position. The changes observed in the solid state isolated from two different solvents (THF and py) are detailed below.

Synthesis. Upon addition of the desired H−OAr to a solution of $LiN(SiMe_3)_2$ dissolved in a Lewis basic solvent (THF or py), an amide−alcohol exchange reaction rapidly occurred to yield the respective "Li(OAr)(solv)$_x$" (eq 3). Each product of eq 3 remained soluble. Upon drastic reduction of the volatile fraction of the reaction mixture and when it is allowed to sit at glovebox temperatures, crystals suitable for X-ray analyses of **1**−**14** were isolated. Analyses that were acceptable within standard variances were not collected for every sample of **1**−**14**, even when rigorous exclusion of air was undertaken. This deviation was attributed to several factors including excess "trapped" solvent, the volatility of the bound solvent, the volatility of the Li ion upon combustion, and the incomplete decomposition forming Li_2CO_3 instead of the presumed Li_2O. The formation of Li_2CO_3 was verified by X-ray diffraction (XRD) analyses of thermally treated materials under an atmosphere of oxygen and calculation of the expected weight loss. The FT-IR spectra of **1**−**14** all possess stretches and bends consistent with THF (**1**−**7**) or py (**8**−**14**) and the appropriate parent alcohol with the notable absence of the OH stretch (3400−3500 cm^{-1}). Stretches of THF or py and the parent alcohol overlap, thereby making it difficult to identify the Li−(μ_x-O) stretches.

To ensure the identity of the bulk powders of the Li(OAr) compounds, alternative analyses were undertaken. Because of the limited analytical data that were available for the previously identified Li(OAr) compounds, $[Li(OPh)(THF)]_6$[17] and $[Li(DBP)(THF)]_2$,[13] it was necessary to synthesize each of these compounds from the reaction mixture of eq 3 and re-solve the structures. The structures adopted for $[Li(OPh)(THF)]_6$ and that found for **1** were not the same (vide infra); however, for **7** and the literature DBP complex, identical structures were recorded but different unit cell parameters were recorded. The py adducts had not been previously reported.

Crystal Structure. Tables 1−3 list the data collection parameters for **1**−**7**, **8**−**14**, and **12b** and **12c**, respectively. Metrical data are presented in Tables 4−8 for **1**−**4**, **5**−**7**, **8**−**11**, **12**−**12c**, and **13** and **14**, respectively. The thermal ellipsoid plots of **1**−**14** are shown in Figures 1−16, respectively. Compounds **2**−**7** were all solved in the *P*2$_1$/*n* or *c* space group with a great deal of structural diversity observed dependent on the ortho substituent. The space groups of the individual py adducts varied considerably for the different substituents, but all of the molecules were isolated as dinuclear species. Additional information pertaining to the structural studies presented here is available in Supporting Information.

The structure of the least sterically hindered aryloxide (OPh) in THF was previously determined to be a tetranuclear cube in solution, but only the hexagonal prismatic structure $[Li(OPh)(THF)]_6$ could be characterized crystallographically.[17] Using the synthetic route described in eq 3, we isolated **1** in a tetranuclear geometry. Because of this difference and the lack of significant structural data available concerning Li(OAr), the other sterically varied Li(OAr) compounds were characterized. A series of H−OAr that demonstrated a stepwise addition of Me, Pr^i, and Bu^t pendant hydrocarbon chains in the ortho position of the phenol ring were investigated (eq 3).

Compounds **1**−**4**, the least sterically hindered OAr ligands investigated, were each found to adopt a cubane structure, [Li-

Table 2. Data Collection Parameters for **8**−**14**

compound	**8**	**9**	**10**	**11**	**12**	**13**	**14**
chemical formula	$C_{32}H_{30}Li_2N_4O_2$	$C_{17}H_{17}LiN_2O$	$C_{36}H_{37}Li_2N_4O_2$	$C_{38}H_{42}Li_2N_4O_2$	$C_{44}H_{54}Li_2N_4O_2$	$C_{20}H_{23}LiN_2O$	$C_{19}H_{26}LiNO$
fw	516.48	272.27	571.58	600.64	684.79	314.34	291.35
temp (K)	168	293	168	168	168	168	188
space group	monoclinic *C*2/*c*	monoclinic *P*2/*c*	orthorhombic *Pna*2$_1$	triclinic $P\bar{1}$	monoclinic *P*2$_1$/*c*	monoclinic *C*2/*c*	monoclinic *P*2$_1$/*c*
a (Å)	18.7700(16)	10.755(2)	18.4842(19)	9.053(2)	11.7494(15)	19.867(2)	9.8461(12)
b (Å)	9.6445(8)	9.463(2)	11.5125(12)	9.746(3)	18.428(2)	9.3926(9)	14.7181(17)
c (Å)	16.4310(14)	16.993(4)	15.3470(17)	11.453(3)	19.100(2)	22.169(2)	12.9470(15)
α (deg)				70.03 (1)			
β (deg)	91.955(2)	93.744(4)		88.09(1)	103.463(2)	115.742(4)	106.38(1)
γ (deg)				70.18(1)			
V (Å^3)	2973(1)	1726(1)	3266(1)	890(1)	4022(1)	3726(1)	1800(1)
Z	4	4	4	1	4	8	4
D_{calcd} (Mg/m^3)	1.154	1.048	1.162	1.121	1.131	1.121	1.075
μ (Mo Kα) (mm^{-1})	0.072	0.065	0.072	0.069	0.068	0.068	0.064
R1[a] (%)	3.86	4.92	8.28	5.18	4.79	4.05	4.21
wR2[b] (%)	10.18	12.50	22.37	11.75	7.04	9.69	10.80
R1[a] (all data, %)	5.65	6.71	19.35	12.72	26.38	6.98	6.84
wR2[b] (all data, %)	11.06	13.48	27.66	14.36	10.47	10.92	11.89

[a] $R1 = \sum||F_o| - |F_c||/\sum|F_o| \times 100$. [b] $wR2 = [\sum w(F_o^2 - F_c^2)^2/\sum(w|F_o|^2)^2]^{1/2} \times 100$.

Table 3. Data Collection Parameters for **12b** and **12c**

compound	**12b**	**12c**
chemical formula	$C_{29}H_{40}LiNO_2$	$C_{39}H_{49}Li_2N_3O_2$
fw	441.56	605.69
temp (K)	168	168
space group	tetragonal $P\bar{4}n2$	monoclinic *P*2$_1$/*n*
a (Å)	12.4605(11)	12.0.965(5)
b (Å)	12.4605(11)	17.665(7)
c (Å)	18.059(2)	16.531(6)
β (deg)		106.95(1)
V (Å^3)	2804(1)	3621
Z	4	4
D_{calcd} (Mg/m^3)	1.046	1.111
μ (Mo Kα) (mm^{-1})	0.064	0.067
R1[a] (%)	4.39	8.53
wR2[b] (%)	10.02	18.49

[a] $R1 = \sum||F_o| - |F_c||/\sum|F_o| \times 100$. [b] $wR2 = [\sum w(F_o^2 - F_c^2)^2/\sum(w|F_o|^2)^2]^{1/2} \times 100$.

$(OAr)(THF)]_4$. This structure is prevalent in alkoxide and alkoxy-like compounds because of the monodentate nature and the free electrons available for the α-oxygen atom.[24] In this structure, each Li atom adopts a distorted tetrahedral geometry with central core angles distorted from the ideal 90°, Li−(μ_3-O)−Li (82.2−87.1°) and (μ_3-O)−Li−(μ_3O) (92.9−97.2°). Additional disorder was noted for the pendant hydrocarbon chains of the alkoxide ligand and the bound solvent. The ortho- and para-substituted $OC_6H_2(2,4,6\text{-}(Me))_3$ derivatives were also reported to adopt a cubane structure; however, one of the Li atoms did not have a bound THF molecule.[19] The Li−(μ_3-O) distances of **1**−**4** (av Li−(μ_3-O) = 1.93 Å (**1**), 1.95 Å (**2**), 2.00 Å (**3**), 1.95 Å (**4**)) are within statistical agreement with each other and with the Li−(μ_3-O) distance of the literature compound $[Li(OPh)(THF)]_6$ (1.99 Å).[17] The longer Li−(μ_3-O) distances noted for **3** are also reflected in longer Li−O_{THF} distances (2.08 Å). For comparison, the Li−O_{THF} distances were on average 1.92 Å for **1**, 1.94 Å for **2**, 1.95 Å for **4**, and 1.96 Å for $[Li(OPh)(THF)]_6$.[17] The longer distances noted for **3** must be a reflection of the increased steric bulk in both ortho positions, which does not allow the ligand to bind as tightly as noted for the other cube structures. This is the first step in the deconstruction of the ubiquitous cube observed for "Li(OAr)(THF)" compounds. For **4**, the Pr^i group is more sterically demanding than the Me groups of **3**. However, because of the asymmetric substitution of the phenoxide ring, **4** adopts an arrangement where the Pr^i group is pointed away from the center of the cube, and thus, steric interactions are minimized.

Increasing the bulk of the ortho substituents to Pr^i groups results in the isolation of a six-membered $[Li-O]_3$ ring complex, **5**, instead of the previously observed cubes (**1**−**4**). This one-dimensional representation of the hexagonal prismatic structure observed for **5** is rare for Li(OR).[24] Only three alternative structures were previously reported as $[Li(OC_6H_2(2,6\text{-}(CH{=}NPr^i))_2(4\text{-}Me))]$,[28] $[Li(OSi(Bu^t)_2OSi(Bu^t)_2F]_3$,[29] and $[Li(OC_6H_2(2,6\text{-}(CH_2NMe_2)_2)(4\text{-}Me)]_3$;[30,24] however, each of those compounds required polydentate ligands or molecular interactions (Li···F interactions) to fill the Li cations coordination sphere. Therefore, **5** is the first example of a "simple" OR adopting this unusual structural motif. The central core of **5** is nearly planar, which forces the Li···Li distance of **5** (av 3.09 Å) to be greater than what was recorded for the cubane compounds (av 2.62 Å, **2**; av 2.70 Å, **3**; 2.64 Å, **4**). The Li−(μ-O) distances of av 1.83 Å for **5** are significantly shorter than those of the Li−(μ_3-O) cubes or the hexagonal prism (vide infra). The terminal Li−O_{THF} distances of **5** (av 1.94 Å) are consistent with those observed for the cubane compounds. The standard trend where the M−O distances increase with increased bonding agrees with the distances observed for **1**−**5**. The regularity of the six-membered ring is reflected in the approximate ideal bond angles of 120 °C noted for **5** (av 119.8 °; range 112.1−128.7°). The trigonal planar arrangement of the Li atoms also allows the terminal THF ligands to adopt angles approaching 120° (av 117.8 °; range 114.7−120.8°).

The introduction of a single but sterically demanding Bu^t group on the phenoxide ring disrupts the ring structure, and a dinuclear compound was isolated for the oBP ligated compound, **6**. This is the most commonly observed structure type for Li(OR) compounds[25] and can be thought of as a one-dimensional representation of the cube. The lithium cation of **6** coordinates two terminal THF molecules, which leads to a tetrahedral arrangement for both Li ions. Substituting both ortho positions with Bu^t groups also leads to a dinuclear complex; however, for **7** only one solvent molecule can bind to the Li metal center.

(28) Korobov, M. S.; Minkin, V. I.; Nivoroshkin, L. E.; Kompan, O. E.; Struchkov, Y. T. *Zh. Obshch. Khim.* **1989**, *59*, 429.
(29) Schmidt-Base, D.; Klingebiel, U. *Chem. Ber.* **1989**, *122*, 815.
(30) van den Schaaf, P. A.; Hogenheide, M. P.; Grove, D.; Spek, A. L.; van Koten, G. *J. Chem. Soc., Chem. Commun.* **1992**, 1703.

Table 4. Select Bond Distances (Å) and Angles (deg) for **1**−**4**

Distances (Å)

	1	**2**	**3**	**4**
Li···Li	Li(1)···Li(2) 2.656(6) Li(1)···Li(1a) 2.631(8) Li(1)···Li(2a) 2.589(5) Li(2)···Li(1a) 2.589(5) Li(2)···Li(2a) 2.585(7)	Li(1)···Li(2) 2.606(10) Li(1)···Li(3) 2.606(1) Li(1)···Li(4) 2.599(10) Li(2)···Li(3) 2.644(10) Li(2)···Li(4) 2.599(10) Li(3)···Li(4) 2.637(11)	Li(1)···Li(2) 2.690(10) Li(1)···Li(3) 2.711(10) Li(1)···Li(4) 2.656(10) Li(2)···Li(3) 2.718(10) Li(2)···Li(4) 2.708(10) Li(3)···Li(4) 2.716(10)	Li(1)···Li(2) 2.676(7) Li(1)···Li(3) 2.563(7) Li(1)···Li(4) 2.636(7) Li(2)···Li(3) 2.648(7) Li(2)···Li(4) 2.640(7) Li(3)···Li(4) 2.659(7)
Li−(μ_3−O)	Li(1)−O(1) 1.933(4) Li(1)−O(2) 1.984(5) Li(1)−O(1a) 1.912(4) Li(2)−O(1) 1.990(4) Li(2)−O(2) 1.922(4) Li(2)−O(2a) 1.907(4) Li(1a)···O(1) 1.912(4) Li(2a)···O(2) 1.907(4)	Li(1)−O(1) 1.974(8) Li(2)−O(1) 1.933(7) Li(4)−O(1) 1.947(8) Li(1)−O(2) 1.947(7) Li(2)−O(2) 1.979(8) Li(3)−O(2) 1.950(8) Li(2)−O(3) 1.958(7) Li(3)−O(3) 1.972(8) Li(4)−O(3) 1.935(7) Li(1)−O(4) 1.926(8) Li(3)−O(4) 1.953(8) Li(4)−O(4) 1.982(8)	Li(1)−O(2) 1.977(7) Li(2)−O(2) 1.971(7) Li(4)−O(2) 2.018(7) Li(2)−O(4) 1.994(7) Li(3)−O(4) 2.046(8) Li(4)−O(4) 1.992(7) Li(1)−O(5) 1.989(7) Li(2)−O(5) 2.033(7) Li(3)−O(5) 1.996(8) Li(1)−O(7) 2.013(7) Li(3)−O(7) 1.970(7) Li(4)−O(7) 1.971(7)	Li(1)−O(1) 1.967(5) Li(2)−O(1) 1.990(5) Li(4)−O(1) 1.990(5) Li(1)−O(2) 1.979(5) Li(3)−O(2) 1.902(5) Li(2)−O(2) 1.980(6) Li(2)−O(3) 1.965(5) Li(3)−O(3) 2.019(6) Li(4)−O(3) 1.915(5) Li(1)−O(4) 1.921(5) Li(3)−O(4) 1.979(5) Li(4)−O(4) 1.969(6)
Li−O_{THF}	Li(1)−O(4) 1.925(4) Li(2)−O(3) 1.912(4)	Li(1)−O(5) 1.958(7) Li(2)−O(6) 1.933(7) Li(3)−O(7) 1.930(8) Li(4)−O(8) 1.928(8)	Li(1)−O(1) 2.018(7) Li(2)−O(3) 2.082(8) Li(3)−O(6) 2.183(8) Li(4)−O(8) 2.027(7)	Li(1)−O(7) 1.948(5) Li(2)−O(8) 1.960(5) Li(3)−O(6) 1.948(6) Li(4)−O(9) 1.955(5)

Angles (deg)

	1	**2**	**3**	**4**
Li−(μ_3-O)−Li	Li(1)−O(1)−Li(1a) 86.33(18) Li(1)−O(1)−Li(2) 85.21(18) Li(1)−O(2)−Li(2) 85.66(17) Li(1)−O(2)−Li(2a) 83.37(16) Li((2)−O(1)−Li(1a) 83.09(17) Li(2)−O(2)−Li(2a) 84.90(17)	Li(1)−O(1)−Li(2) 83.4(3) Li(1)−O(1)−Li(4) 83.0(3) Li(2)−O(1)−Li(4) 83.8(3) Li(1)−O(2)−Li(2) 83.2(3) Li(1)−O(2)−Li(3) 83.9(3) Li(2)−O(2)−Li(3) 84.6(3) Li(2)−O(3)−Li(3) 84.6(3) Li(2)−O(3)−Li(4) 83.8(3) Li(3)−O(3)−Li(4) 84.9(3) Li(1)−O(4)−Li(3) 84.4(3) Li(1)−O(4)−Li(4) 83.4(3) Li(3)−O(4)−Li(4) 84.2(3)	Li(1)−O(2)−Li(2) 85.9(3) Li(1)−O(2)−Li(4) 83.3(3) Li(1)−O(5)−Li(2) 83.9(3) Li(1)−O(5)−Li(3) 85.8(3) Li(1)−O(7)−Li(3) 85.8(3) Li(1)−O(7)−Li(4) 83.6(3) Li(2)−O(2)−Li(4) 85.5(3) Li(2)−O(4)−Li(3) 84.5(3) Li(2)−O(4)−Li(4) 85.6(3) Li(2)−O(5)−Li(3) 84.9(3) Li(3)−O(4)−Li(4) 84.5(3) Li(3)−O(7)−Li(4) 87.1(3)	Li(1)−O(1)−Li(2) 85.1(2) Li(1)−O(1)−Li(4) 83.5(2) Li(1)−O(2)−Li(2) 85.0(2) Li(1)−O(2)−Li(3) 82.6(2) Li(1)−O(4)−Li(3) 82.2(2) Li(1)−O(4)−Li(4) 85.3(2) Li(2)−O(1)−Li(4) 83.1(2) Li(2)−O(2)−Li(3) 86.0(2) Li(2)−O(3)−Li(3) 83.3(2) Li(2)−O(3)−Li(4) 85.7(2) Li(3)−O(3)−Li(4) 85.0(2) Li(3)−O(4)−Li(4) 84.7(2)
(μ_3-O)-Li−(μ_3−O)	O(1)−Li(1)−O(1a) 93.21(18) O(1)−Li(1)−O(2) 94.12(18) O(1)−Li(2)−O(2a) 96.73(17) O(1)−Li(2)−O(2) 94.27(18) O(2)−Li(1)−O(1a) 96.76(18) O(2)−Li(2)−O(2a) 94.68(17)	O(1)−Li(1)−O(2) 96.4(3) O(1)−Li(1)−O(4) 97.0(4) O(1)−Li(2)−O(3) 95.6(3) O(1)−Li(4)−O(3) 96.2(3) O(1)−Li(4)−O(4) 96.0(3) O(2)−Li(2)−O(1) 96.4(3) O(2)−Li(2)−O(3) 94.9(3) O(2)−Li(1)−O(4) 96.0(3) O(2)−Li(3)−O(3) 95.4(3) O(2)−Li(3)−O(4) 95.0(3) O(3)−Li(3)−O(4) 95.1(4) O(3)−Li(4)−O(4) 95.3(3)	O(2)−Li(1)−O(5) 95.4(3) O(2)−Li(1)−O(7) 96.5(3) O(2)−Li(2)−O(4) 94.8(3) O(2)−Li(2)−O(5) 94.2(3) O(2)−Li(4)−O(4) 93.4(3) O(2)−Li(4)−O(7) 96.5(3) O(4)−Li(2)−O(5) 95.4(3) O(4)−Li(3)−O(5) 95.0(3) O(4)−Li(3)−O(7) 93.1(3) O(4)−Li(4)−O(7) 94.8(3) O(5)−Li(1)−O(7) 93.4(3) O(5)−Li(3)−O(7) 94.5(3)	O(1)−Li(1)−O(2) 94.9(2) O(1)−Li(1)−O(4) 96.2(2) O(1)−Li(2)−O(2) 94.1(2) O(1)−Li(2)−O(3) 94.6(2) O(1)−Li(4)−O(3) 96.2(2) O(1)−Li(4)−O(4) 94.0(2) O(2)−Li(1)−O(4) 97.2(2) O(2)−Li(2)−O(3) 94.8(2) O(2)−Li(3)−O(3) 95.5(2) O(2)−Li(3)−O(4) 97.8(2) O(3)−Li(3)−O(4) 92.9(2) O(3)−Li(4)−O(4) 96.6(2)
O_{THF}−Li−(μ_3-O)	O(3)−Li(2)−O(1) 125.3(2) O(3)−Li(2)−O(2a) 119.9(2) O(3)−Li(2)−O(3) 119.0(2) O(4)−Li(1)−O(1) 120.1(2) O(4)−Li(1)−O(1a) 120.7(2) O(4)−Li(1)−O(2) 124.6(2)	O(5)−Li(1)−O(1) 123.7(4) O(5)−Li(1)−O(2) 122.5(4) O(5)−Li(1)−O(4) 115.2(4) O(6)−Li(2)−O(1) 115.2(4) O(6)−Li(2)−O(2) 126.1(4) O(6)−Li(2)−O(3) 122.0(4) O(7)−Li(3)−O(2) 118.1(4) O(7)−Li(3)−O(3) 124.5(4) O(7)−Li(3)−O(4) 121.9(4) O(8)−Li(4)−O(1) 122.4(4) O(8)−Li(4)−O(3) 115.5(4) O(8)−Li(4)−O(4) 124.9(4)	O(1)−Li(1)−O(2) 101.8(3) O(1)−Li(1)−O(5) 122.1(4) O(1)−Li(1)−O(7) 137.7(4) O(3)−Li(2)−O(2) 112.8(3) O(3)−Li(2)−O(4) 107.3(3) O(3)−Li(2)−O(5) 142.4(4) O(6)−Li(3)−O(4) 140.6(4) O(6)−Li(3)−O(5) 108.4(3) O(6)−Li(3)−O(7) 115.4(3) O(8)−Li(4)−O(2) 138.2(4) O(8)−Li(4)−O(4) 122.3(4) O(8)−Li(4)−O(7) 101.0(3)	O(6)−Li(3)−O(2) 123.0(3) O(6)−Li(3)−O(3) 131.7(3) O(6)−Li(3)−O(4) 107.6(2) O(7)−Li(1)−O(1) 123.5(3) O(7)−Li(1)−O(2) 109.6(2) O(7)−Li(1)−O(4) 128.1(3) O(8)−Li(2)−O(1) 135.7(3) O(8)−Li(2)−O(2) 117.5(3) O(8)−Li(2)−O(3) 111.4(3) O(9)−Li(4)−O(1) 112.9(3) O(9)−Li(4)−O(3) 132.4(3) O(9)−Li(4)−O(4) 116.9(3)

It was necessary to re-solve the structure of **7** because of the absence of analytical data previously presented in the initial report and the isolation of crystalline material with a unit cell and space group different from those previously reported.[13] The Li−(μ-O) and Li···Li distances of **6** (1.91 and 2.53 Å, respectively) and **7** (1.82 and 2.39 Å, respectively) are significantly shorter than those noted for **1**−**5** but in agreement with literature metrical data. The steric bulk of the Bu^t group limits the amount of electron density available to the Li metal center; thus, a stronger interaction between the Li and O atoms occurs, resulting in shorter Li−O distances. Compound **7**, which has only one coordinated THF molecule, displays even shorter Li−O distances than **6** because of the reduction in electron donation by the coordinated solvents. Other reported structures of OAr

Table 5. Select Bond Distances (Å) and Angles (deg) for **5**−**7**

Distances (Å)

	5	**6**	**7**
Li···Li	Li(1)···Li(2) 3.162(8) Li(1)···Li(3) 3.048(8) Li(2)···Li(3) 3.060(8)	Li(1)···Li(1a) 2.527(6)	Li(1)···Li(1a) 2.382(9) Li(2)···Li(2a) 2.399(8)
Li−(μ_x-O)	Li(1)−O(1) 1.830(6) Li(1)−O(3) 1.844(6) Li(2)−O(1) 1.822(6) Li(2)−O(2) 1.807(6) Li(3)−O(2) 1.846(6) Li(3)−O(3) 1.829(6)	Li(1)−O(1) 1.907(3) Li(1)−O(1a) 1.911(3) Li(1a)···O(1) 1.911(3)	Li(1)−O(1) 1.822(4) Li(2)−O(2) 1.816(4)
Li−O_{THF}	Li(1)−O(4) 1.937(6) Li(2)−O(5) 1.958(6) Li(3)−O(6) 1.920(6)	Li(1)−O(2) 2.002(3) Li(1)−O(3) 2.014(3)	Li(1)−O(4) 1.891(5) Li(2)−O(3) 1.883(4)

Angles (deg)

	5	**6**	**7**
Li−(μ_x-O)−Li	Li(1)−O(1)−Li(2) 119.9(3) Li(2)−O(2)−Li(3) 113.8(3) Li(3)−O(3)−Li(1) 112.1(3)	Li(1)−O(1)−Li(1a) 82.90(13)	Li(1)−O(1)−Li(1a) 80.5(2) Li(2)−O(2)−Li(2a) 81.1(2)
(μ_x-O)−Li−(μ_x−O)	O(1)−Li(1)−O(3) 122.5(3) O(1)−Li(2)−O(2) 121.8(3) O(2)−Li(3)−O(3) 128.7(3)	O(1)−Li(1)−O(1a) 97.10(13)	O(1)−Li(1)−O(1a) 99.5(1) O(2)−Li(2)−O(2a) 98.9(2)
O_{THF}−Li−(μ_x−O)	O(1)−Li(1)−O(4) 116.7(3) O(1)−Li(2)−O(5) 118.9(3) O(2)−Li(2)−O(5) 119.3(3) O(2)−Li(3)−O(6) 116.1(3) O(3)−Li(1)−O(4) 120.8(3) O(3)−Li(3)−O(6) 114.7(3)		O(1)−Li(1)−O(4) 130.2(2) O(1a)−Li(1)−O(4) 130.2(2) O(2)−Li(2)−O(3) 136.1(2) O(2a)−Li(2)−O(3) 125.0(2)

Table 6. Select Bond Distances (Å) and Angles (deg) for **8**−**11**

Distances (Å)

	8	**9**	**10**	**11**
Li···Li	Li(1)···Li(1a) 2.620(4)	Li(1)··· ···Li(1a) 2.58(6)	Li(1)···Li(2) 2.547(13)	Li(1)···Li(1a) 2.552(6)
Li−(μ-O)	Li(1)−O(1) 1.900(2) Li(1)−O(1a) 1.890(2)	Li(1)−O(1) 1.902(3) Li(1)−O(1a) 1.896(3)	Li(1)−O(1) 1.881(9) Li(1)−O(2) 1.896(10) Li(2)−O(1) 1.891(10)	Li(1)−O(1) 1.914(4) Li(1)−O(1a) 1.885(3)
Li−N	Li(1)−N(1) 2.079(2) Li(1)−N(2) 2.083(2)	Li(1)−N(1) 2.098(3) Li(1)−N(2) 2.137(4)	Li(1)−N(3) 2.147(10) Li(1)−N(4) 2.123(9) Li(2)−N(1) 2.088(11) Li(2)−N(2) 2.157(10)	Li(1)−N(1) 2.135(4) Li(1)−N(2) 2.086(4)

Angles (deg)

	8	**9**	**10**	**11**
Li−(μ-O)−Li	Li(1)−O(1)−Li(1a) 87.43(8)	Li(1)−(O1)−Li(1a) 85.64(14)	Li(1)−O(2)−Li(2) 84.0(4) Li(1)−O(1)−Li(2) 84.9(5)	Li(1)−O(1)−Li(1a) 84.41(15)
(μ-O)−Li−(μ-O)	O(1)−Li(1)−O(1a) 92.57(8)	O(1)−Li(1)−O(1a) 94.36(14)	O(1)−Li(1)−O(2) 95.9(4) O(1)−Li(2)−O(2) 95.2(4)	O(1)−Li(1)−O(1a) 95.59(15)
(μ-O)−Li−N	O(1)−Li(1)−N(1) 107.17(9) O(1)−Li(1)−N(2) 118.67(10)	O(1)−Li(1)−N(1) 116.67(17) O(1)−Li(1)−N(2) 109.10(15)	O(1)−Li(1)−N(3) 124.4(5) O(1)−Li(1)−N(4) 111.6(5) O(2)−Li(1)−N(3) 117.6(5) O(2)−Li(1)−N(4) 115.2(4) O(1)−Li(2)−N(1) 110.3(5) O(1)−Li(2)−N(2) 128.0(6) O(2)−Li(2)−N(1) 114.6(6) O(2)−Li(2)−N(2) 109.0(5)	O(1)−Li(1)−N(1) 109.90(16) O(1)−Li(1)−N(2) 117.20(17)
N−Li−N	N(1)−Li(1)−N(2) 108.22(9)	N(1)−Li(1)−N(2) 110.00(14)	N(1)−Li(2)−N(2) 100.5(4) N(3)−Li(1)−N(4) 93.5(4)	N(1)−Li(1)−N(2) 109.14(15)

ligands with substitutions in the para position, such as [Li(OC$_6$H$_2$(2,6-(Bu^t))$_2$(4-Me)(OEt$_2$)]$_2$,[9] did not further decrease the nuclearity of the observed products.

For **8**−**13**, the compounds adopt an edge-shared fused tetrahedral arrangement consisting of two bridging OAr ligands and two terminal py solvent ligands, forcing each Li atom into the ubiquitous distorted tetrahedral arrangement. The Li−(μ-O) distances of the py adducts (av 1.90 Å, **8**; 1.90 Å, **9**; 1.90 **10**; 1.90 Å, **11**; 1.89 Å, **12**; 1.91 Å, **13**) are slightly longer than those distances observed for the THF adducts, but the Li···Li distances of the pyridine adducts are significantly shorter. The Li−N distances of the pyridine adducts are self-consistent, and the central [Li−O]$_2$ rings of **8**−**13** are nearly planar with Li−O−Li angles that are ∼15−20 ° smaller than the O−Li−O angles.

Table 7. Select Bond Distances (Å) and Angles (deg) for **12**, **12b**, and **12c**

Distances (Å)

	12	**12b**	**12c**
Li···Li	Li(1)···Li(2) 2.448(7)		Li(1)···Li(2) 1.820(8)
Li−(μ-O)	Li(1)−O(1) 1.855(5) Li(1)−O(2) 1.883(5) Li(2)−O(1) 1.930(5) Li(2)−O(2) 1.898(5)	Li(1)−O(1) 1.818(3) Li(1)−O(1a) 1.818(3)	Li(1)−O(1) 1.942(7) Li(1)−O(2) 1.830(7)
Li−N_{py}	Li(1)−N(1) 2.231(6) Li(1)−N(4) 2.083(5) Li(2)−N(2) 2.185(5) Li(2)−N(3) 2.080(5)	Li(1)−N(1) 2.072(5)	Li(1)−N(1) 2.082(6) Li(1)−N(3) 2.110(6) Li(2)−N(2) 2.048(7)

Angles (deg)

	12	**12b**	**12c**
Li−(μ-O)−Li	Li(1)−O(1)−Li(2) 80.6(2) Li(1)−O(2)−Li(2) 80.6(2)		Li(1)−O(1)−Li(2) 81.7(3) Li(1)−O(2)−Li(2) 81.9(3)
(μ-O)−Li−(μ-O)	O(1)−Li(1)−O(2) 96.7(2) O(1)−Li(2)−O(2) 93.7(2)	O(1)−Li(1)−O(1a) 116.9(2)	O(1)−Li(1)−O(2) 94.1(3) O(1)−Li(2)−O(2) 102.4(3)
(μ-O)−Li−N_{py}	O(1)−Li(1)−N(1) 122.2(3) O(1)−Li(1)−N(4) 125.3(3) O(2)−Li(1)−N(1) 100.9(2) O(2)−Li(1)−N(4) 115.5(3) O(1)−Li(2)−N(2) 105.7(2) O(1)−Li(2)−N(3) 120.6(2) O(2)−Li(2)−N(2) 123.3(2) O(2)−Li(2)−N(3) 111.5(2)	O(1)−Li(1)−N(1) 121.57(12) O(1a)−Li(1)−N(1) 121.57(12)	O(1)−Li(1)−N(1) 111.9(3) O(1)−Li(1)−N(3) 108.3(3) O(2)−Li(1)−N(1) 116.1(3) O(2)−Li(1)−N(3) 112.8(3) O(1)−Li(2)−N(2) 125.3(4) O(2)−Li(2)−N(2) 125.1(4)
N_{py}−Li−N_{py}	N(1)−Li(1)−N(4) 94.8(2) N(2)−Li(2)−N(2) 103.2(2)		N(1)−Li(1)−N(3) 112.1(3)

Table 8. Select Bond Distances (Å) and Angles (deg) for **13** and **14**

Distances (Å)

	13	**14**
Li···Li	Li(1)···Li(1a) 2.412(4)	Li(1)···Li(1a) 2.417(4)
Li−(μ-O)	Li(1)−O(1) 1.908(2) Li(1)−O(1′) 1.916(2)	Li(1)−O(1) 1.887(2) Li(1)−O(1a) 1.815(2)
Li−N_{py}	Li(1)−N(1) 2.088(2) Li(1)−N(2) 2.141(2)	Li(1)−N(1) 2.030(2)

Angles (Å)

	13	**14**
Li−(μ-O)−Li	Li(1)−O(1)−Li(1a) 78.23(10)	Li(1)−O(1)−Li(1a) 81.49(10)
(μ-O)−Li−(μ-O)	O(1)−Li(1)−O(1a) 100.29(9)	O(1)−Li(1)−O(1a) 98.51(1)
(μ-O)−Li−N_{py}	O(1)−Li(1)−N(1) 113.99(10) O(1)−Li(1)−N(2) 112.68(10) O(1a)−Li(1)−N(1) 123.02(11) O(1a)−Li(1)−N(2) 104.50(9)	O(1)−Li(1)−N(1) 124.11(11)
N_{py}−Li−N_{py}	N(1)−Li(1)−N(2) 102.30(9)	

Two unusual derivatives of the DIP ligated species were isolated as $[Li(DIP)(py)(H\text{-}DIP)]_2$ (**12b**) and $[Li_2(DIP)_2(py)_3]$ (**12c**). Analytical data on **12b** and **12c** were not gathered because of the difficulty in isolating these compounds in a rational synthetic pathway; however, the unusual structural features are of interest. Compound **12b** was isolated from a similar reaction stoichiometry reported for **12**, but surprisingly, an H-DIP solvent molecule was coordinated to the metal wherein each Li atom is tricoordinated with a bridging DIP, terminal py, and one terminal H-DIP ligand. This ligand supplies electron density and enough steric bulk to fill the Li's coordination sphere, forming a monomeric complex; however, hydrogen bonding between the individual molecules act as a bridge between the monomers, yielding a dimeric molecule. The bond distances of **12b** are consistent with those noted for the other analogues.

Attempts to synthesize **12b**, independently, using a stoichiometric amount of H-DIP were unsuccessful. Instead, the asymmetric molecule **12c**, was isolated with two distinct Li environments. The molecule consists of two Li atoms bridged by DIP ligands; however, one Li is tetrahedral with two coordinated py solvent molecules and the other is trigonal planar with only one coordinated py molecule. The metrical data of **12** and **12c** are in agreement with each other and the other "Li(OAr)$(py)_x$" compounds. However, both compounds possess one M−N bond distance that is significantly longer than the other M−N distances. For **12**, the packing diagrams reveal py ligands that are interlaced with sufficient space for each solvent ligand; however, in **12c** the molecules are arranged in such a manner that no additional py ligands can be incorporated into the structure. One of the DIP ligands of **12c** is bent, hindering the introduction of an additional py ligand; however, the influences that bend the DIP ligand are not fully understood to date. It is important to note that **12c** was grown from an H-DIPP/py solution whereas **12** was isolated from a py solution, and this difference may be enough of an influence to elicit this unusual structure.

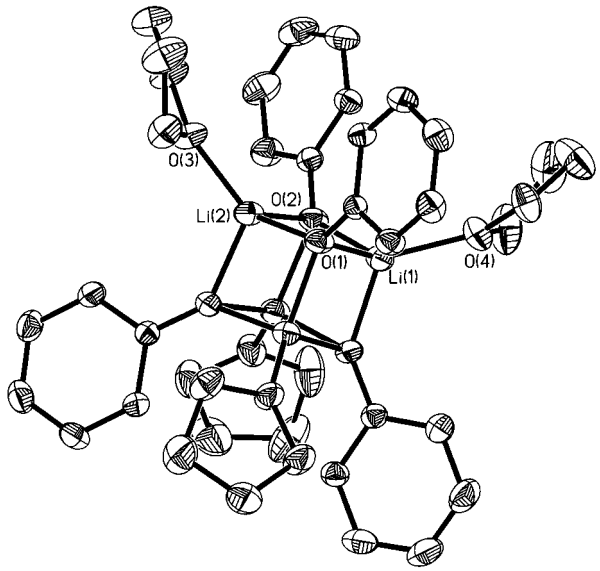

Figure 1. Thermal ellipsoid plot of **1**. Ellipsoids are drawn at the 30% probability level.

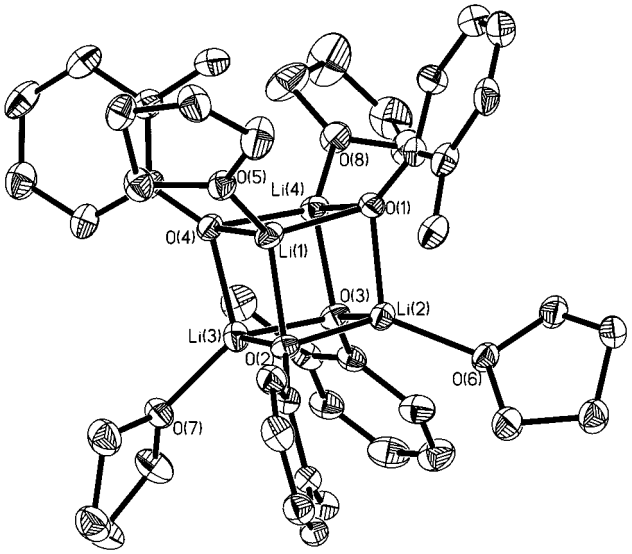

Figure 2. Thermal ellipsoid plot of **2**. Ellipsoids are drawn at the 30% probability level.

Compound **14** is also dinuclear, but only one py is bound to each Li cation. This can be attributed to the steric bulk of the butyl substituents, which forces the Li atoms into a distorted trigonal planar geometry, as was noted for the tricoordinated Li metal center of $[Li(OC_6H_2(2,6\text{-}(Bu^t))_2(4\text{-}Me)(OEt_2)]_2$[9] and **5**.

Solid-State NMR. For **1**−**14**, a ^{13}C MAS NMR spectrum was collected and the chemical shifts tabulated in Table 9. For each sample, one set of ^{13}C resonances was observed for the respective ligands; however, several peaks in these sets were found as multiplets. The nonequivalent resonances were attributed to packing differences, hindered rotation of the ligands, and the disorder noted in the crystal structure for various "Li(OAr)(solv)$_x$" compounds. While a more detailed study is necessary to fully quantitate these spectra, some preliminary trends can be elucidated.

For the THF adducts, it was observed that as the OAr substituent increases in size and as the nuclearity of the molecule decreases, the ^{13}C NMR chemical shift of the methyl substituent is shifted further downfield (**2**, 17.2; **3**, 18.4; **4**, 22.1; **5**, 21.8; **6**, 30.0; **7**, 31.5 ppm). The ^{13}C chemical shifts of the methyl resonances of the py adducts also follow the same general trend (except for **14**); there is no change in the Li coordination or the nuclearity of the resultant products: δ 17.8 ppm for **9**, 18.6 ppm for **10**, 24.1 ppm for **11**, 23.8 ppm for **12**, 30.4 ppm for **13**, and 30.4 ppm for **14**. The shifts in the methyl resonances of the various OAr for **1**−**14** do not follow any trends in terms of the metrical Li−O bond distances (Table 9), and thus, this reflects the negligible influence of the Li cations on the ^{13}C chemical shifts of the substituents. The solid-state structures of **1**−**14** are symmetric, and thus, it is not possible from the respective ^{13}C MAS NMR spectra to determine the nuclearity of the bulk powder. Therefore, alternative nuclei were used to further confirm the identity of the bulk powder.

The ^{6}Li MAS NMR spectra for compounds **1**−**14** are shown in Figure 17. For the solid-state $^{6,7}Li$ MAS NMR, $\pi/6$ pulses

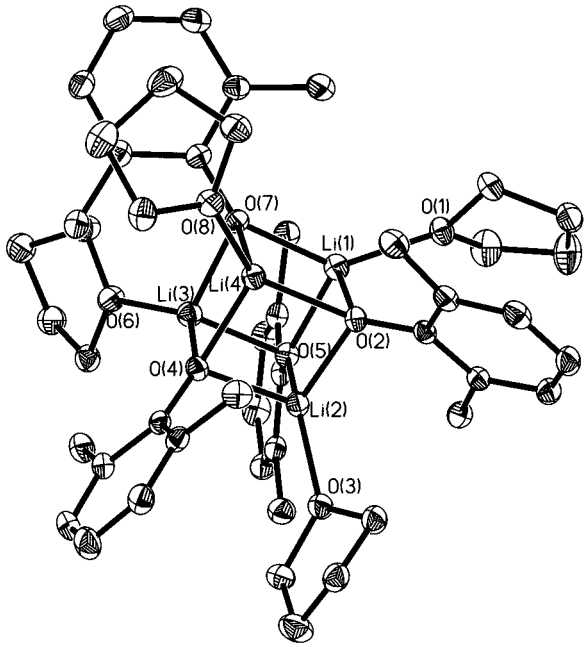

Figure 3. Thermal ellipsoid plot of **3**. Ellipsoids are drawn at the 30% probability level.

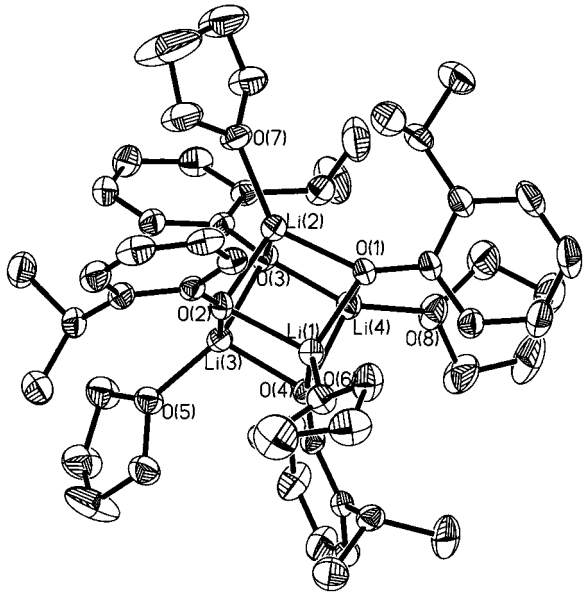

Figure 4. Thermal ellipsoid plot of **4**. Ellipsoids are drawn at the 30% probability level.

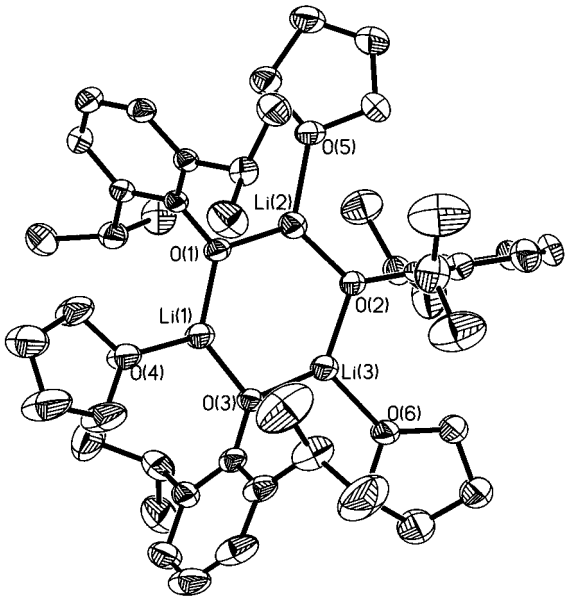

Figure 5. Thermal ellipsoid plot of **5**. Ellipsoids are drawn at the 30% probability level.

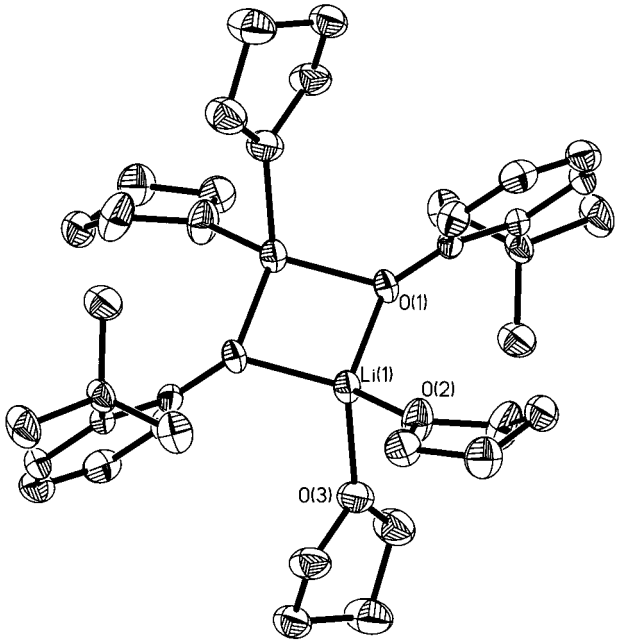

Figure 6. Thermal ellipsoid plot of **6**. Ellipsoids are drawn at the 30% probability level.

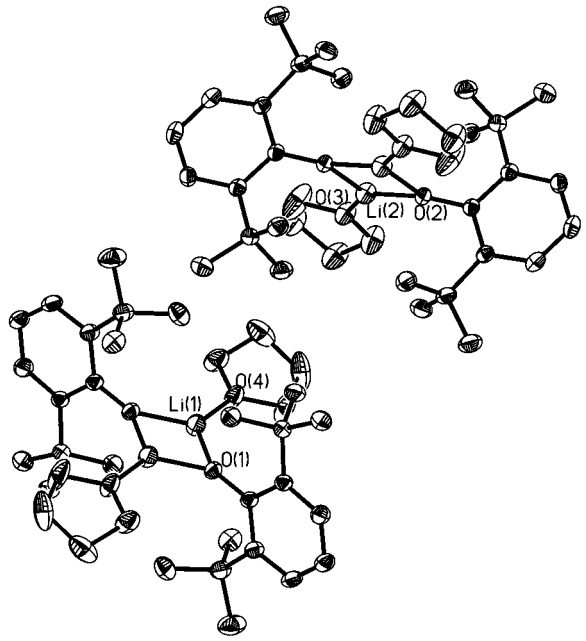

Figure 7. Thermal ellipsoid plot of **7**. Ellipsoids are drawn at the 30% probability level.

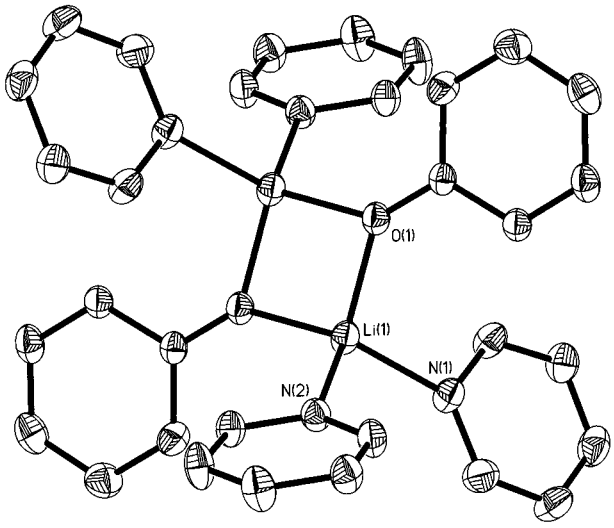

Figure 8. Thermal ellipsoid plot of **8**. Ellipsoids are drawn at the 30% probability level.

were used to ensure adequate excitation if significant quadrupolar interactions were present. Recycle delays varied from 1 to 60 s in order to ensure sufficient time for complete spin−lattice relaxation. In the solid state the ^{6}Li chemical shift is equal to the true isotropic chemical shift (since the second-order quadrupolar shift is negligible for ^{6}Li) and is used to discuss changes in structure. The Li chemical shift is a function of the local environment around the metal and is influenced by both the number of neighboring coordinating anions and their respective distances. Secondary effects on the observed Li chemical shift due to the nature and spatial arrangement of the surrounding cations within the structure has also been noted.[31,32] Most of the ^{6}Li resonances recorded for **1**−**14** are asymmetric and could be deconvoluted into several overlapping resonances. For the discussion here, only the frequency of the peak maximum is recorded. While the chemical shift range for Li NMR is quite small (<10 ppm), some general trends have been observed based on the limited data collected.

The spectra of **1**, **2**, and **6** show a broad, nonresolved set of resonances. The overlapping resonances observed in both the ^{6}Li and the ^{13}C MAS NMR spectrum of **1** most likely reflect packing inequivalencies coupled with the multiple Li environments for different structural types (cube and hexagonal prism) observed for this compound. Compounds **2** and **6** possess shoulders on the main resonance, but these are not well defined. Compound **3** displayed two distinct ^{6}Li resonances. The remainder of the samples revealed a single resonance that would be consistent with the symmetric solid-state structures; however, it is of note that computer deconvolution hints at the presence of multiple nuclei.

The ^{6}Li chemical shifts for **1**−**4**, which all possessed Li cations in distorted Td in the crystal structure, had resonances

(31) Alam, T. M.; Conzone, S.; Brow, R. K.; Boyle, T. J. *J. Non-Cryst. Solids* **1999**, *258*, 140.
(32) Xue, X.; Stebbins, J. F. *Phys. Chem. Miner.* **1993**, *20*, 297.

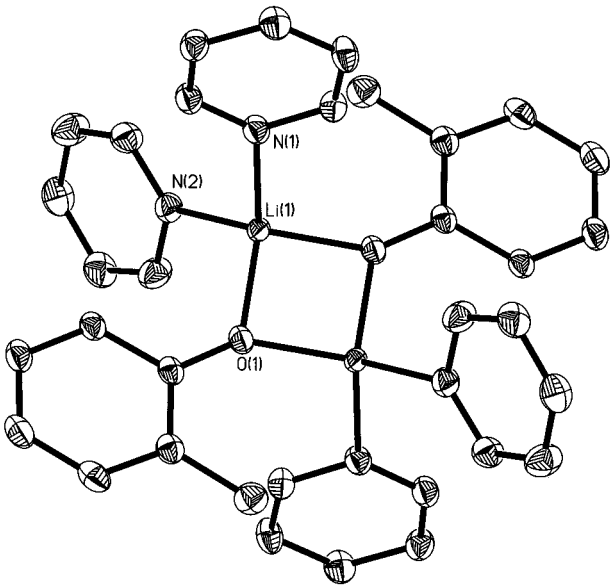

Figure 9. Thermal ellipsoid plot of **9**. Ellipsoids are drawn at the 30% probability level.

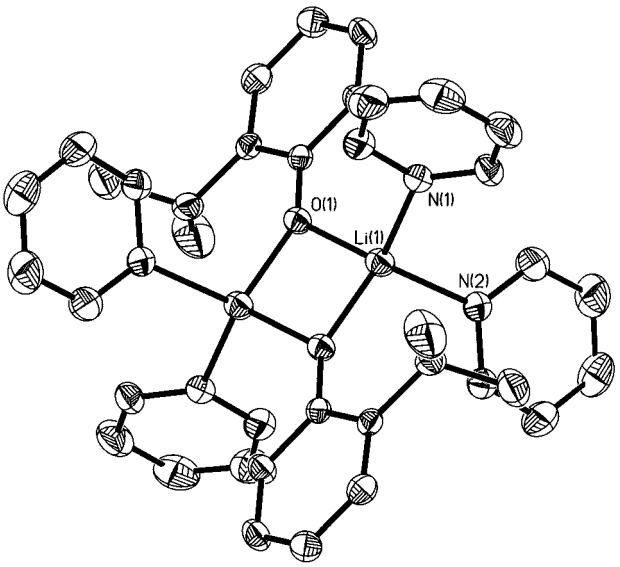

Figure 11. Thermal ellipsoid plot of **11**. Ellipsoids are drawn at the 30% probability level.

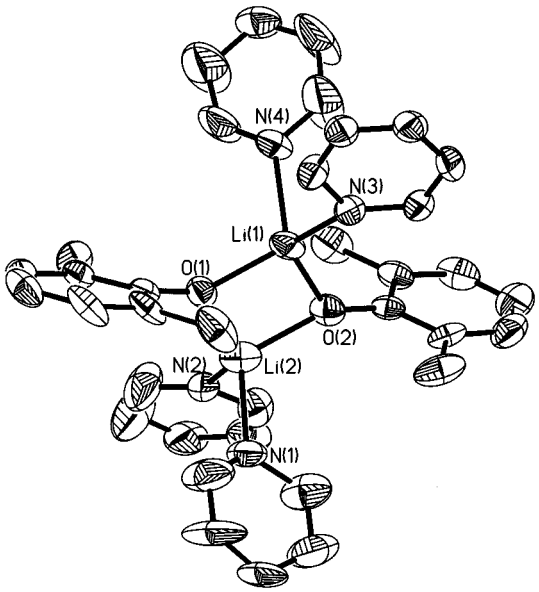

Figure 10. Thermal ellipsoid plot of **10**. Ellipsoids are drawn at the 30% probability level.

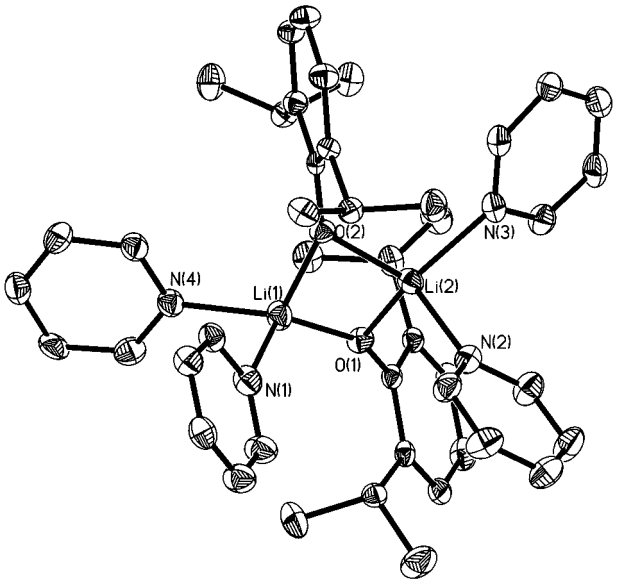

Figure 12. Thermal ellipsoid plot of **12**. Ellipsoids are drawn at the 30% probability level.

clustered around ~0.6 ppm. The distorted trigonal geometries of the Li in **5** and **7** were found further upfield around 0.41 and 0.51 ppm, respectively. The resonance at 2.02 ppm observed for **2** is further downfield than that of any of the other observed resonances and remains unassigned. The chemical shifts of the expected decomposition products, Li_2O (δ 2.8, 1.3, 0.31), LiOH (δ 1.22, 0.31), or Li_2CO_3 (δ 0.02) do not correspond to this additional resonance. The shift of the dinuclear compound **6** is significantly varied from all of the other samples, displaying negative shifts. Structurally, **6** possesses Td bound Li atoms but is the only compound with two THF ligands bound to the metal center in the solid state.

The ^{7}Li (spin $^3/_2$) MAS spectra for **1**−**14** are shown in Figure 18 and are dominated by the central $\pm^1/_2$ to $\pm^1/_2$ transition, but a manifold of spinning sidebands for the $\pm^3/_2$ to $\pm^1/_2$ transition is also clearly evident. The extent of this sideband manifold provides a measure of the quadrupolar coupling constant, and the data are listed in Table 9. The quadrupolar coupling constant (also known as SOQE or QSC) is defined by $P_Q = C_Q(1 + (\eta_Q)^2/3)^{1/2}$, where $C_Q = e^2qQ/h$ is the quadrupolar coupling constant and η_Q is the quadrupolar electrical field gradient asymmetry parameter. The experiments and analysis described here do not allow for C_Q and η_Q to be separated. Because $0 \leq \eta_Q \leq 1$, C_Q and P_Q differ at most by 15%. The P_Q value is used as an indication of asymmetry around the Li cations (i.e., large P_Q values indicate less symmetry around the Li cation).

As can be discerned from the data, there are two distinct regions of P_Q values that directly correlate with the coordination number of the Li atom. The values below 150 kHz are consistent with tetracoordinated Li metal centers, and those values above 250 kHz are consistent with tricoordinated metal centers. Jackmann et al. reported a solid-state P_Q value of only 73 kHz for $[Li(OPh)(THF)]_6$.[17] While we have described our sample of **1** as a mixture of both the tetra- and hexanuclear species, several other experimental variables may also contribute to the differences in the observed ^{7}Li line shape (i.e., the size of P_Q), including our use of MAS, high spinning speeds, and high power

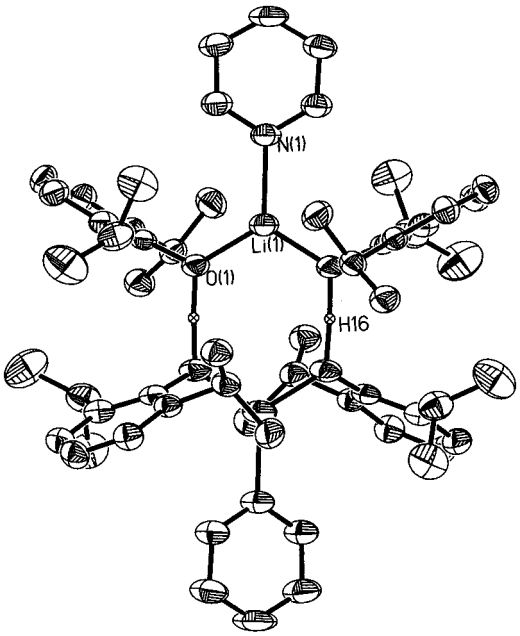

Figure 13. Thermal ellipsoid plot of **12b**. Ellipsoids are drawn at the 30% probability level.

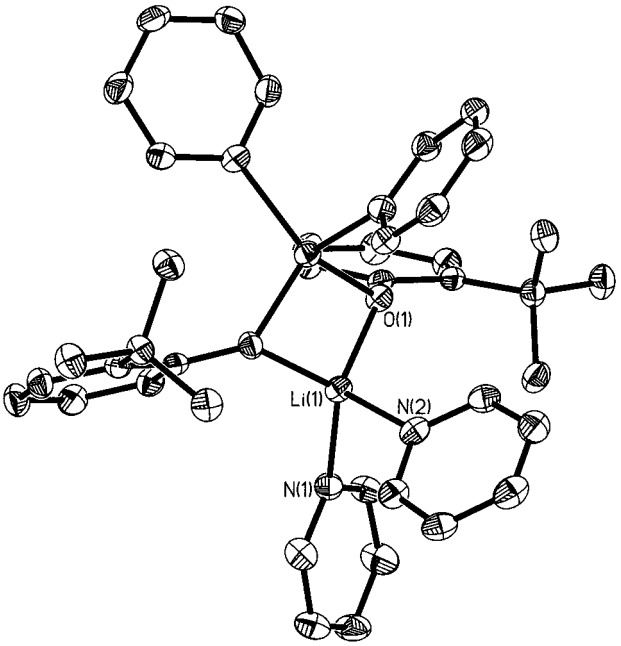

Figure 15. Thermal ellipsoid plot of **13**. Ellipsoids are drawn at the 30% probability level.

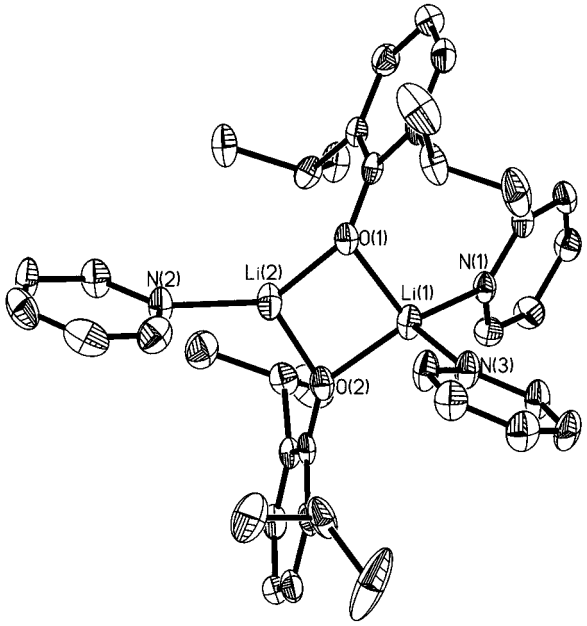

Figure 14. Thermal ellipsoid plot of **12c**. Ellipsoids are drawn at the 30% probability level.

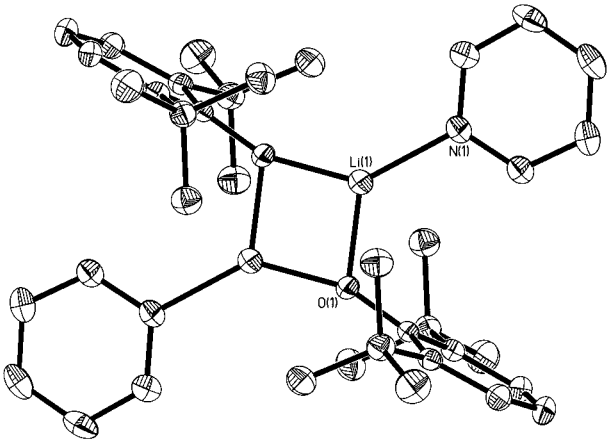

Figure 16. Thermal ellipsoid plot of **14**. Ellipsoids are drawn at the 30% probability level.

excitation pulses to obtain a larger excitation bandwidth. It may also be possible that the 73 kHz value reported by Jackmann et al. represents a P_Q that has been partially motionally averaged (a smaller QSC indicates higher dynamical averaging).[17] The QSC values noted for $LiPO_3$, which also has tetracoordinate Li, were found to be 110 kHz[31] which is consistent with the values reported for the "Li(OAr)(solv)" compounds in Table 9.

For **5** and **7**, the large quadrupolar coupling observed (~1000 ppm) implies that a very asymmetric Li environment exists for these compounds, in contrast to **1**−**4** and **6**. The increased symmetry observed for the other compounds may reflect a highly symmetric bonding environment or partial averaging of the quadrupolar interaction due to dynamics of the Li. Comparison of the shifts observed in the ^{6}Li and ^{7}Li MAS experiments can also provide a measure of the quadrupolar interaction, but the absence of any significant shift (within experimental error) indicates that the quadrupolar interaction is rather small for most of these compounds.

Interestingly, the compounds that display multiple Li environments (**1** and **3**) may be on the verge of changing from one structure to another geometry (or "structural transition" ligated species). For **1**, the transition of the hexagonal prismatic structure to the cube arrangement has already been reported. Therefore, it is not unreasonable to expect a similar transition from a cube to a ring arrangement. While the two Me substituents of **3** impose some very large steric constraints, as evidenced by the metrical data, it was found to adopt the cube structure. It is quite possible that both a ring and cube arrangement are present, explaining the observed spectra; however, only the cube structure was crystallographically isolated.

Figures 17 and 18 show the ^{6}Li and ^{7}Li solid-state MAS NMR spectra, respectively, of the py adducts **8**−**14** with the peak maxima of these compounds tabulated in Table 9. The ^{6,7}Li NMR data collected on these samples reveal only one resonance for every sample. These single resonances are consistent with the symmetrical environments observed in the solid-state

Table 9. Solid-State MAS and Solution NMR Data for **1**−**14**

compd	δ ^{7}Li[a]	δ ^{13}C{^{1}H} MAS	δ ^{6}Li MAS	δ ^{7}Li[b] MAS	^{7}Li P_Q (kHz)[c]	MC[d]	CN[e]	Li−Solv[f] (av)	ref
1	1.26(1)	167.0,162.9, 128.9, 119.5,118.5, 114.3, 57.0(THF), 24.6(THF)	0.58(5), −0.11(5)	0.2(1)	120	4	4	1.93	*g*
						6	4	1.96	*8*
2	1.15(1)	165.3, 129.9, 127.3, 118.8, 114.3, 67.6 (THF), 25.0 (THF), 17.2	0.62(5)	0.8(2)	50	4	4	1.95	*g*
3	0.64(1)	163.4, 129.4, 126.9, 123.7, 113.4, 68.5(THF), 26.1, 25.0(THF), 18.4	0.56(5) (2.02(5))	0.7(1)	70	4	4	2.00	*g*
4	1.65(1) (1.34(1))	163.7, 162.6, 161.2, 135.9, 135.0, 127.7, 125.3, 118.9, 116.3, 67.3(THF), 25.3(THF), 22.1	0.55(5)	0.6(1)	50	4	4	1.95	*g*
5	0.70(1)	161.3, 136.0, 123.5, 122.4, 116.5, 114.7, 68.0(THF), 25.5(THF), 21.8	0.41(5)	0.5(1)	275	4	3	1.83	*g*
6	0.35(1)	168.7, 164.4, 136.9, 125.2, 115.3, 111.5, 67.9(THF), 34.5, 30.0, 26.1(THF)	−0.25(5)	−0.1(1)	140	2	4	1.91	*g*
7	0.90(1)	165.1, 138.2, 136.8, 125.1, 112.9, 112.0, 100.1, 68.2(THF), 35.4, 31.5, 25.2(THF)	0.51(5)	0.1(1)	260	2	3	1.82	*g*
						2	3	1.85	15
8	2.90(1)	167.8, 149.2(py), 138.5(py), 136.4(py), 128.4, 124.9, 119.8, 113.9	2.02(5)	1.9(1)	60	2	4	1.90 2.08	*g*
9	3.29(1)	165, 150.4(py), 136.8(py), 132.4, 127.8, 124.1(py), 118.5, 114.6, 17.8	1.26(5)	1.3(1)	25	2	4	1.90 2.11	*g*
10	3.06(1)	165.7, 161.0, 150.9(py), 136.6(py), 128.4, 127.0, 123.9(py), 115.2, 113.6, 18.6	1.59(5)	1.7(1)	50	2	4	1.89 2.13	*g*
11	3.31(1)	167.5, 148.7(py), 137.5(py), 126.9, 125.7, 123.3(py), 119.8, 110.7, 24.8, 24.1	2.35(5)	1.7(1)	25	2	4	1.90 2.11	*g*
12	2.78(1)	160.7, 149.0(py), 138.2(py), 137.1, 135.9(py), 125.3, 123.2(py), 113.5, 27.3, 23.8	1.03(5)	1.1(1)	250	2	4	1.89 2.14	*g*
13	2.43(1)	169.6, 149.1(py), 136.6(py), 126.7, 125.6, 123.7(py), 110.9, 35.7, 30.4	1.96(5)	1.6(1)	100	2	4	1.91 2.11	*g*
14	3.02(1)	165.4, 148.4(py), 139.7, 138.8(py), 125.1,124.3(py), 113.5, 35.8, 30.4	1.53(5)	1.2(1)	270	2	3	1.85 2.03	*g*

[a] Solution NMR for **1**−**7** in THF-d_8 and for **8**−**14** in py-d_5. [b] Peak maximum, not corrected for quadrupolar shift effects. [c] Quadrupolar coupling product was estimated from the width of the spinning sideband manifold and has an error of about ±10 kHz. [d] MC = molecular complexity. [e] CN = coordination number. [f] Solv = THF for **1**−**7**. Solv = py for **8**−**14**. [g] This work.

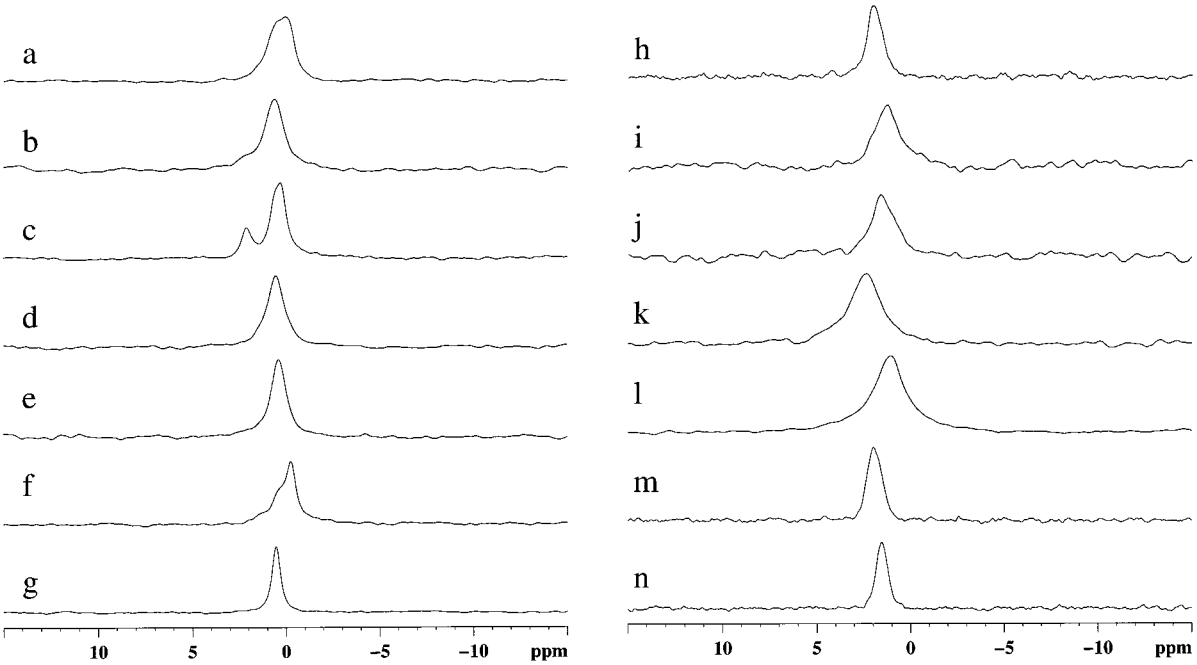

Figure 17. Solid-state ^{6}Li MAS NMR spectra of **1**−**14** (spectra a−n, respectively).

structures. For the ^{6,7}Li MAS experiments of compounds **12** and **14**, very large spinning sideband manifolds were found in comparison to the remainder of py coordinated compounds. The reduction of the quadrupolar interaction in **8**−**11** and **13** reflects a high symmetry in the Li environment or an averaging of the quadrupolar interaction by Li dynamics.

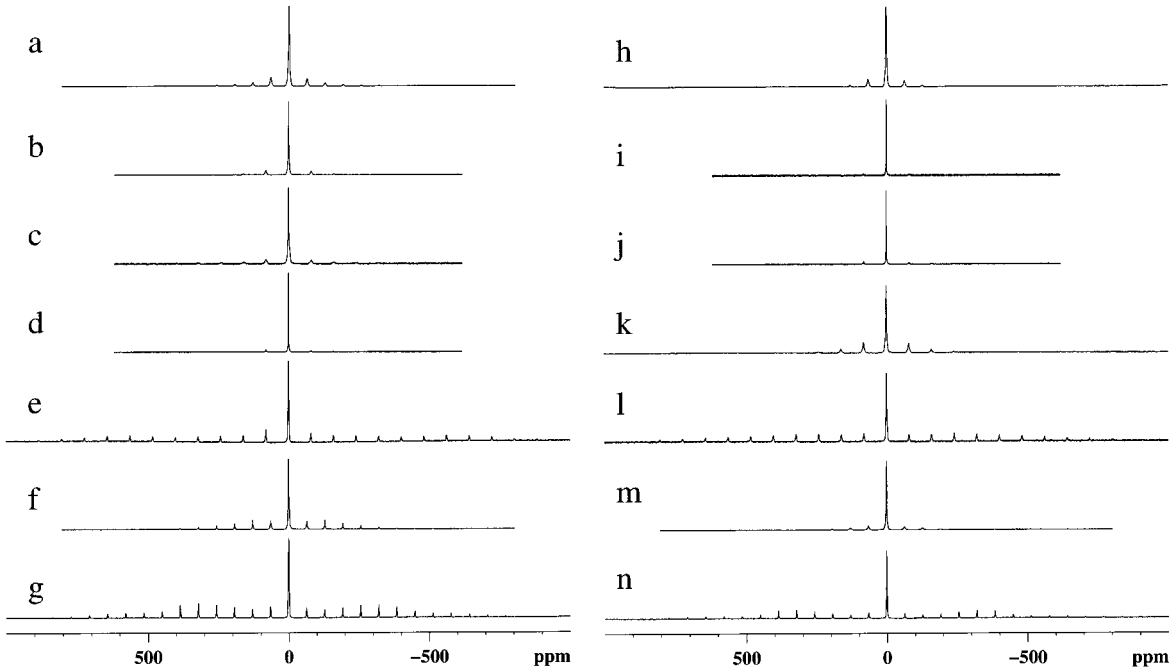

Figure 18. Solid-state ^{7}Li NMR spectra of **1**−**14** (spectra a−n, respectively).

In contrast to the THF adducts, a smaller ^{6}Li chemical shift range was observed for **8**−**14**. The py compounds are all dinuclear, and there is little evidence of transitional structure changes occurring in **8**−**14**. This lack of transitional structures must be a reflection of the strength of the Lewis basicity of the bound py, or better π-donating ability, that supplies sufficient electron density to minimize oligomerization. The lack of multiple resonances for any of the $[Li(OAr)(py)_x]_2$ adducts in the ^{6}Li MAS NMR spectra suggests that a limited number of structural species are accessible when using strong Lewis basic solvents. As noted for the THF adducts, no correlation between bond distance and coordination number can be made concerning these compounds. Again, two distinct regions of P_Q values for **8**−**14** that directly correlate with the coordination number of the Li atom are shown. The values below 150 kHz are consistent with tetracoordinated Li^0 metal centers, and those values above 250 kHz are consistent with tricoordinated metal centers. The only exception to this trend is **12**, which may be a reflection of the multiple structural arrangements (**12b** and **12c**) that we have characterized for **12**.

Solution State. Previously, Jackmann and co-workers have reported a series of elegant investigations regarding the solution nuclearity of Li(OAr) compounds in a variety of solvents.[15−17] The conclusions reached on the THF derivatives that overlap with this investigation indicated that in a THF solution at −60 °C the OPh (**1**) molecule was a mixture of tetranuclear/hexanuclear,[15] the oMP (**2**) derivative was a tetranuclear,[16] and the oBP (**6**) analogue was dinuclear.[16] This is consistent with the solid-state structures observed in this study. It was also determined from Jackmann et al.'s work that in py, at −60 °C, the OPh (**8**) compound existed as a tetrameric species, the DMP (**10**) was dinuclear with two solvent molecules, and the DBP (**14**) was mononuclear (or oligomeric).[15] In an effort to correlate our solid-state results with the reported solution results, a series of multinuclear NMR experiments were undertaken. For these studies, all samples were prepared using a crystalline material dissolved in THF-d_8 or py-d_5 at saturated concentrations at room temperature. It is difficult to judge the number of solvent molecules as they relate to the solid-state structure, because of the use of deuterated parent solvent to maximize solubility and minimize exchange. Alternative solvents were not investigated.

For compounds **1**−**14**, the solution ^{1}H and $^{13}C\{^{1}H\}$ NMR spectra displayed only one set of resonances for each of the individual ligands. Variable temperature NMR spectra that would assist in understanding the solution behavior of these compounds could not be collected because of the propensity of these compounds to precipitate upon cooling at the concentrations that we were investigating. Therefore, Li NMR studies were initiated.

^{7}Li NMR is a very sensitive method for determining the environment of the Li cation, and in solution the quadrupolar interactions are effectively averaged to zero. In general, the nearest-neighbor coordination environment controls the Li chemical shift with secondary effects noted on the basis of the nature and spatial arrangement of the surrounding cations within the structure. For the high-resolution ^{7}Li NMR, recycled delays were varied from 5 to 60 s to ensure complete relaxation between acquisitions. The solution spectra are shown in Figure 19 for the THF and py adducts. The shifts of these compounds are quite varied from the solid-state structures and reflect changes in the local bonding environment of the Li atom either by disruption of the structure or by solvent effects. Again, only the frequency of the peak maximum is recorded while detailed peak deconvolutions were not pursued.

For **1**, two peaks are present, which is consistent with the Li cation environments observed in the hexagonal prismatic and cube structures previously reported.[17] The resonance consistent with the cube was also observed as the only peak for **2** but as a minor peak for **4**. Compound **4** also displays a peak that correlates with the hexagonal prismatic resonance observed for **1**. For the disubstituted species (**3**, **5**, and **7**), each has a ^{7}Li NMR resonance around 0.6 ppm, which may indicate that monomeric species exist in solution. For **6**, the Li chemical shift is at 0.35 ppm and may be at the low end of the range of shifts noted for dinuclear species. For **8**−**14**, only one resonance is observed in each case, ranging from δ 2.41 to δ 3.31. The chemical shifts of these samples fall within a relatively small range, which indicates that the metal centers are all in similar

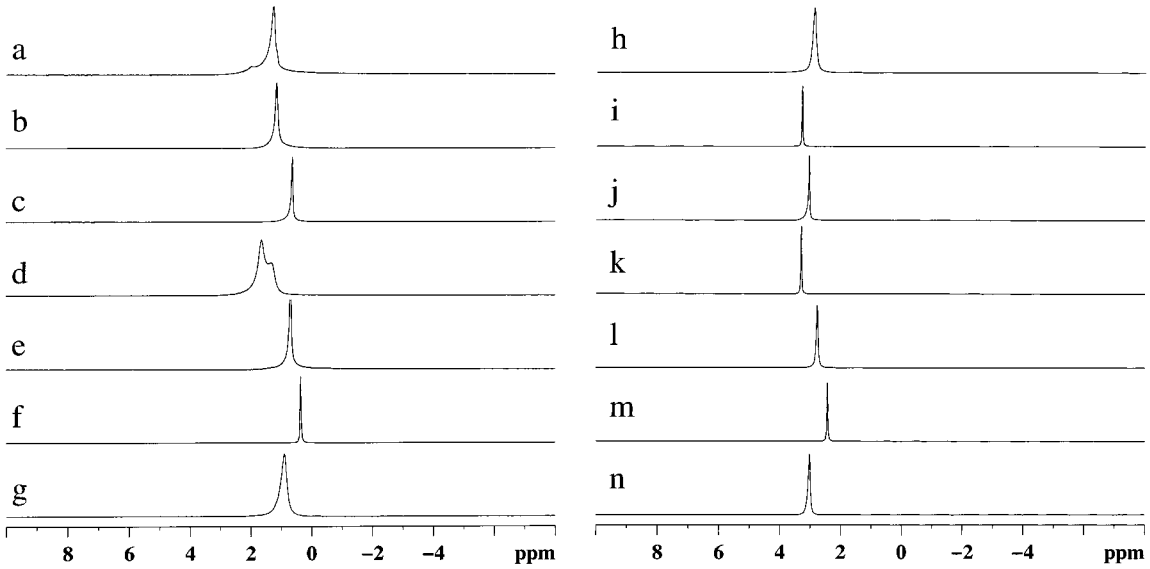

Figure 19. Solution-state ^{7}Li NMR spectra of **1**−**7** (spectra a−g, respectively) in THF-d_8 and **8**−**12** (spectra h−n, respectively) in py-d_5.

environments. The symmetrically substituted species appear in the middle and the asymmetric OAr ligands (oMP, oPP, and oBP) ligated species occupy the extremes. Substantially more work is necessary to definitively determine the actual structural species present in solution, but as has been noted previously,[15−17] there appears to be a great deal of fluctional behavior with rapid exchange of ligands and structure types.

Summary and Conclusion

A number of sterically varied "Li(OAr)(solv)$_x$" precursors have been identified by single-crystal X-ray diffraction and ^{6,7}Li NMR spectroscopy. The structures of the THF adducts oscillate between six- and four-membered rings of Li−O atoms of various dimensions (hexagonal prism to a cube to a hexagon to a square) as the steric bulk of the ortho substituent is increased. For the "Li(OAr)(py)$_x$" complexes (**8**−**14**), dinuclear geometries, independent of the steric interactions of the phenol ring, were the only structures observed. The introduction of the sterically demanding disubstituted *tert*-butyl groups leads only to loss of a solvent molecule per metal center, yet mononuclear species were not observed. Two additional unusual structures **12b** and **12c** were isolated for the DIP ligand. While rational syntheses of these compounds do not exist yet, on the basis of the similarities of structures observed for **8**−**14**, it is not unreasonable to believe that these compounds may also exist for each of these compounds.

Solid-state ^{6}Li MAS NMR was used to characterize the bulk powders of **1**−**14**. As evidenced by broad peaks and computer deconvolution, more than one Li environment may be represented for a number of the THF ligated samples. In particular, **1** and **3** reveal multiple Li environments and may be considered "structural transition" ligated species. On the basis of metrical data, compound **4** should also be considered a transitional ligated species but only a single resonance was observed. For the ^{6,7}Li MAS NMR spectra of **8**−**14**, single resonances were observed within a very small chemical shift range. This indicates a consistency of Li environments, which would be in line with the reported crystal structures. In solution, a single ^{7}Li NMR resonance was observed for **1**−**14** except for **4**, which displayed multiple resonances. The multiple nuclei observed for **4** further verify the structural transition of **4**. However, conclusions based on the molecularity of these solution species will require more investigation to positively assign the observed resonances.

Interestingly, we have not been able to obtain a monomeric solid-state "Li(OAr)(solv)" complex using these monodentate solvents and ligands. However, as has been shown, the use of multidentate ligands or polydentate solvents will achieve this goal, but these ligands greatly hinder the metathesizability of the Li metal.[24] Therefore, alternative electron-donating substituents on the OAr rings or even stronger Lewis basic solvents are under consideration to generate a complex more amenable to metathetical synthetic approaches. Because of the fluctionality in structural arrangements, it should be possible to use the steric bulk of the substituent to control the solution and solid-state structures, resulting in a fine-tuning of the Li−O bond strength and thus the ultimate reactivity of the Li(OAr) in methathical processes.

Acknowledgment. For support of this research, the authors thank the Office of Basic Energy and Science and the United States Department of Energy under Contract DE-AC04-94AL85000. Sandia is a multiprogram laboratory operated by Sandia Corporation, a Lockheed Martin Company, for the United States Department of Energy.

Supporting Information Available: Experimental details and characterization of **1**−**14** and X-ray crystallographic files in CIF format for the structures of [Li(OAr)(THF)$_x$]$_n$ (**1**−**7**) and [Li(OAr)(py)$_x$]$_n$ (**8**−**14**).This material is available free of charge via the Internet at http://pubs.acs.org.

IC000432A